Modeling of Earthquake Induced Pore Pressure and Submarine Slope Stability Analysis

Rajib Dey & Bipul Hawlader
Memorial University of Newfoundland, St. John's, NL, Canada
Ryan Phillips
C-CORE, St. John's, NL, Canada
Kenichi Soga
University of Cambridge, United Kingdom

ABSTRACT
A method to analyze submarine slope stability during an earthquake is presented in this paper. The angles of most submarine slopes are very gentle and therefore the analysis has been performed assuming them as infinite slopes. In this study, the soils involved in slope failure are contractive loose to medium dense sands. It has been shown that both earthquake induced inertia force and pore water pressure in sand layer play a critical role in slope stability. The loose sand layers may not always be continuous in an offshore slope. Considering the end forces on the sliding block a method is presented to calculate the minimum length of the loose to medium dense sand layer required to fail the slope at a given depth. An energy based model (Berrill and Davis 1985) has been used to estimate the pore water pressure generated during an earthquake. The Berrill and Davis model has been further verified using additional case histories of liquefaction.

RÉSUMÉ
Une méthode pour analyser la stabilité des talus sous-marin pendant un tremblement de terre est présenté dans le présent document. Les angles de la plupart des pentes sous-marines sont très doux et donc l'analyse a été effectuée en les considérant comme une pente infinie. Dans cette étude, les sables impliqués dans une rupture de pente sont considéré comme contractant (lâches). Il a été montré que les séismes peuvent à ;a fois induiren une force d'inertie et des pressions interstitielles dans une couche de sable lesquelles jouent un rôle crucial dans la stabilité des pentes. Les couches de sable peuvent ne pas être toujours continues dans les talus au large des côtes. Considérant les forces à la limite des blocsqui glissent,, une méthode est présentée pour calculer la longueur minimale de la couche de sable lâche requise rupture du talus à une profondeur donnée. Un modèle basé sur l'énergie (Berrill et Davis 1985) a été utilisé pour estimer la pression d'eau interstitielle produite lors d'un séisme. Le modèle de Berrill et Davis a, de plus, été vérifié à l'aide d'histoires de cas deliquéfaction.

1 INTRODUCTION

The stability of sloping seafloors is an important issue that must be considered in the design of offshore facilities such as offshore pipelines, foundations and wellheads. The consequences of slope failure could have a large financial, safety and regulatory impact. Numerous failures of submarine slopes have been reported in the literature; some of them are small while some are very large such as Storegga slide in the Norwegian Sea or Grand Banks slide in offshore Newfoundland. The submarine slides may be initiated by a variety of potential triggering factors such as earthquakes, rapid sedimentation, wave action, gas hydrate dissociation, diapirism, artesian water pressure, oversteeping by erosion and minor slides, human activities, tide, sea level change, glaciations and volcanic activities (Locat and Lee 2002, Masson et al. 2006). Among them earthquakes have been considered one of the major causes of submarine landslides. Pore water pressure generated from earthquake shaking could reduce the shear strength of soil significantly and cause the failure of a submarine slope (Wright et al. 2003, Kvalstad et al. 2005).
A submarine slope might fail during and also after earthquake shaking. The response of the slope depends on the magnitude of the earthquake, soil properties and geometry of the slope. During the earthquake, seismic induced inertia force creates some additional shear stress on the potential failure plane. Seismic excitation can also generate pore water pressure in some soil, such as loose sand, which can reduce the shear strength of the soil along the failure plane. The excess pore water pressure cannot be significantly dissipated during the earthquake as it happens in a very short period of time and therefore the analysis should be performed considering the effects of excess pore water pressure (Hadj-Hamou et al. 1985, Biondi et al. 2000).
This paper presents a method to analyze the stability of submarine slopes subjected to earthquake. The soil considered is loose to medium sand, which loses its shear strength due to the generation of excess pore water pressure. The pore water pressure has been estimated using an energy-based pore pressure model. The pore water pressure generation models have been reviewed and the model used in this study has been verified with some additional data.
A submarine slope might also fail after the earthquake shaking. One reason could be the presence of thin silt layer of low permeability above the loose sand deposit under which a water film could be developed by post-

liquefaction void redistribution (Kokusho 2003) as demonstrated by Coulter and Phillips (2005). However, this type of failure is not discussed in this paper. It is also to be noted here that many submarine landslides occurred in clayey deposits (Masson et al. 2006, Brink et al. 2009). However, the present study focused mainly on failure in sand.

2 STABILITY OF AN INFINITE SLOPE UNDER EARTHQUAKE LOAD

Consider a long continuous submarine slope with an inclination of β as shown in Fig. 1. Typically submarine slopes are very gentle having a slope angle (β) less than 10° (Hadj-Hamou et al. 1985). The slope is stable under the static shear stress (τ_{static}) caused by the gravitational force. An earthquake in this area might cause the failure of this slope.

Extremely loose sand is not very common in the seabed because other environmental effects such as wave loading increase the soil density. If the slope is in the earthquake prone area, earthquakes of small intensity may not cause the failure of the slope. However, pore pressure will be generated due to these earthquakes which will be dissipated with time and densify the soil. This is known as "seismic strengthening" (Lee et al. (2004). Coulter and Phillips (2005) successfully modelled the seismic strengthening behaviour using geotechnical centrifuge. Therefore, in this study it is assumed that the soil involved in potential failure of the slope is loose sand not very loose sand.

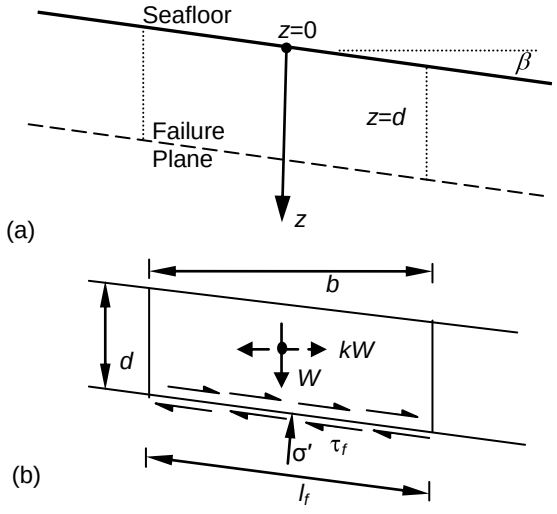

Figure 1: (a) Geometry of slope (b) Stress state

The simplest analysis of the stability of a submarine slope can be performed by assuming it as an infinite slope with a failure plane parallel to the sea floor. Let us assume a potential failure plane at depth *d* as shown in Fig. 1. If the length of the failure plane (l_f) is significantly greater than *d*, it can be considered as an infinite slope. Whether this slope will fail due to an earthquake or not depends upon the soil behaviour along the potential failure surface. The soil behaviour of loose sand is described in the following section.

3 BEHAVIOUR OF LOOSE AND COMPACT SAND AND ITS IMPLICATION TO SLOPE FAILURE

Typical behaviour of saturated contractive sand is shown schematically in Fig. 2. The point A represents the initial stress state of a soil element in the slope. The soil element is in drained equilibrium under the static shear stress (τ_{static}) and the slope in the field is stable under this stress. If this soil specimen is sheared monotonically from this initial condition in triaxial cell in undrained condition, it will follow the stress path ABC as shown in Fig. 2. Shear stress continues to increase to the peak at point B where it becomes unstable and further increase in pore water pressure strains the soil elements rapidly to the residual shear strength (τ_r) at point C. Undrained strain softening is triggered only if the static shear stress (τ_{static}) is greater than residual shear strength (τ_r). If the same specimen is loaded cyclically in undrained condition the soil element becomes unstable at point D and then follows similar strain-softening response from D to C. It should be noted that a significant shear strain occurs during the path from B to C (in case of monotonic load) or D to C (in case of cyclic load) than that of in A to B or A to D (Fig. 2b). Although the effective stresses at point B and D are different, all these points fell in one line OB as shown in Fig. 2a (Kramer 1996; Hanzawa 1980).

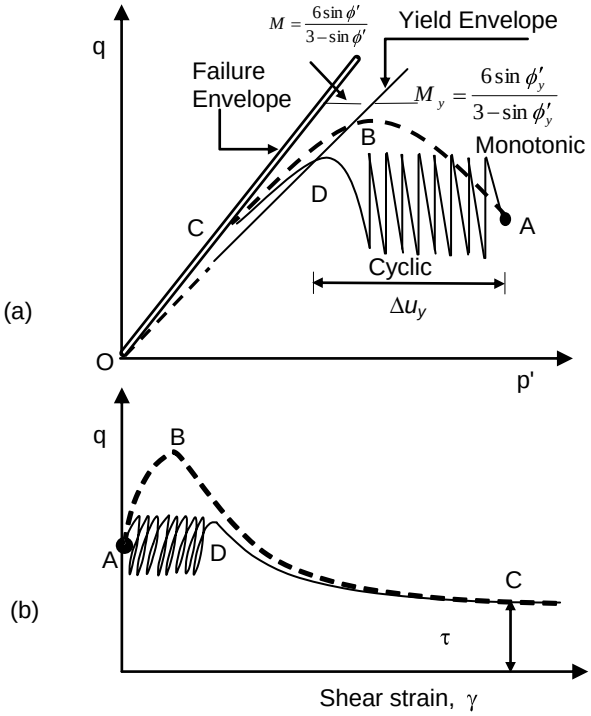

Figure 2: Behaviour of sand under monotonic and cyclic loads

Various names have been given for this line including *yield strength envelope* (Hanzawa 1980, Olson and Stark 2003), *flow liquefaction surface* (Vaid and Chern

1985,Yang 2002), *collapse surface* (Sladen et al. 1985), *instability line* (Lade and Yamamuro 2011, Chu et al. 2003), and *peak strength envelop* (Poulos 1988). In this study, the term "yield strength envelope" is used to represent this condition and the corresponding friction angle is referred as "yield friction angle, ϕ'_y."

If the pore water pressure generated from an earthquake reduces the effective stress to the yield envelope the soil sample becomes imminent to collapse. Collapse of soil structure results in strain-softening behaviour as shown in Fig. 2(b). The slope of the yield and failure envelopes could be obtained from conventional geotechnical laboratory tests. The yield strength envelope is not unique but depends upon the void ratio or relative density and confining pressure. The slope of the yield strength line (M_y) could be low for very loose sand while it could be same or very close to the slope of the critical state line (M) for higher relative densities (Sladen et al. 1985, Chu et at. 2003). In general, the slope of the yield envelope in triaxial compression is higher than that of in simple shear tests (Olson and Startk 2003, Terzaghi et al. 1996). In most of the submarine slope failures the mode of shear on the potential failure plane corresponds approximately to the simple shear condition. Lade and Yamamuro (2011) also pointed out that slope of the yield strength envelope from anisotropically (K_0) consolidated specimen is higher than that of isotropically consolidated specimen of the same void ratio. Therefore, the difference between the failure line and yield envelopes may not be very high in offshore environment since the soil is anisotropically consolidated and subsequently compacted by environmental loads. However, as the soil is still in loose state collapse after yield is possible. Therefore, the analysis should be also performed considering the residual shear strength at point C. Note that, if the static shear stress is less than the residual shear strength, the stress path can travel beneath the point C without reaching to any collapse surface (Kramer 1996). However, such a low shear stress in not considered in this study.

4 STABILITY ANALYSIS

Limit equilibrium analysis is generally performed for stability analysis of a slope. When the shear stress on the potential failure plane exceeds the shear strength of soil at that plane the slope fails. Shear stress could be generated from variety of sources, however only the gravitational and earthquake induced shear stresses are considered in this study.

Referring to Fig. 1(b) the following expression can be written for normal (σ_0') and shear (τ_0) stresses at the base of the sliding block.

$$\sigma'_0 = \gamma' d \cos^2\beta \quad \text{and} \quad \tau_0 = \gamma' d \sin\beta\cos\beta \qquad [1]$$

Seismic excitation will have at least two effects on slope stability. During an earthquake excess pore water pressure (Δu) might be generated in the soil near the sliding surface. The excess pore water pressure cannot be dissipated during a very short period of earthquake duration. It will reduce the normal effective stress to σ_0'-Δu, which in turn reduce the shear strength significantly. The driving force will be also increased by earthquake shaking. Similar to pseudostatic screening analysis, the earthquake induced horizontal force can be modelled using a horizontal earthquake coefficient (k_h). Note that, in pure pseudostatic analysis earthquake induced pore water pressure is not considered and is suitable for stability analysis of slopes when the soil involved are not expected to lose their shear strength significantly during earthquake shaking (Makdisi and Seed 1977). However, the soil considered here is loose sand; both effects need to be considered to scrutinize the shear strength reduction (Azizian and Popescu, 2001, Hadj-Hamou et al. 1985).

Therefore the factor of safety (F_s) of a given infinite slope can be written as:

$$F_s = \frac{(1 - r_u)\tan\phi'_y}{\tan\beta + k_h\gamma_t/\gamma'} \qquad [2]$$

where γ' and γ_t are the submerged and total unit weight of the soil above the failure plane, respectively; r_u ($= \Delta u/\sigma'_0$) is the pore pressure ratio; and ϕ'_y is the yield friction angle.

5 EFFECTS OF SOIL LAYER ABOVE THE FAILURE PLANE

The effects of the upper soil layer above the failure plane AB in Fig. 3 have not been considered in the factor of safety calculation discussed in section 4. It has been assumed that the length of the failure plane is infinite and therefore the resistance offered by the soil above the failure plane is negligible. However, in offshore environment the soil layer involved in failure may not be homogeneous and the zone of loose contractive sand, where the failure could be initiated, may not be continuous. Several questions may arise regarding the effect of upper soil layer on slope failure such as: (i) At what depth the failure could be initiated? (ii) What is the minimum length of the weak soil layer required to initiate a failure at that depth? (iii) How does the failure propagate through the upper soil layer? (iv) How to model that propagation? A simplified modeling procedure is presented in the following sections to answer these questions.

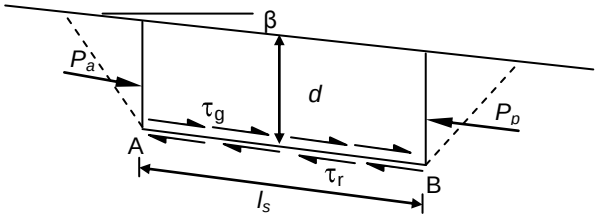

Figure 3: Slope with a finite length of weak zone

Consider a long continuous submarine slope (Fig. 3) with an inclination of β similar to Fig. 1. This time the weak contractive sand layer is not infinite but of a finite length of l_s. The sliding of the soil block is possible only if the driving force is greater than the resistance offered by the loose

sand layer at the bottom and as well as two end zones. The situation at the upper and lower ends of the sliding block is very similar to the active and passive earth pressure conditions, respectively.

Based on Mazindrani and Ganjali (1997), P_p -P_a can be calculated as;

$$P_p - P_a = \frac{2d^2\gamma' \cos^2\beta\left(-r_{u1}\sqrt{\left(\cos^2\beta - \cos^2\phi_1'\right)}\right)}{\cos^2\phi_1'} \qquad [3]$$

where P_a and P_p are the active and passive forces, respectively, ϕ_1' is the angle of internal friction of the soil layer above the failure zone, and r_{u1} is the pore pressure ratio in that layer. Note that, if the stress-strain behaviour of the upper soil layer is similar to the behaviour presented in Fig. 2, $\phi_1' = \phi_y'$ should be used. Otherwise, for example for medium to dense sand, the critical state friction angle should be used.

Using the equilibrium condition of the sliding block in Fig. 3, the factor of safety (F_s) can be calculated as

$$F_s = \frac{\tau_r l_s + P_p}{\tau_g l_s + P_a}, \qquad [4]$$

where $\tau_g (= \gamma' d \cos\beta \sin\beta + k_h \gamma_t d \cos^2\beta)$ is the sum of the shear stresses resulting from gravitational and earthquake induced force and τ_r is the residual strength. If the excess pore pressure ratio is known, the residual shear strength τ_r can be also calculated as (see Fig. 2)

$$\tau_r = \gamma' d \cos^2\beta (1 - r_u) \tan\phi_{cs}' \qquad [5]$$

Therefore, the minimum length l_s required to cause the failure of a slope at a depth d can be obtained by putting F_s =1 in Eq. (4).

$$l_s = \frac{P_p - P_a}{\tau_g - \tau_r} \qquad [6]$$

Now replacing the values of τ_g and τ_r as discussed above, the Eq. (6) can be rewritten as:

$$l_s = \frac{2d\left(-r_{u1}\sqrt{\left(\cos^2\beta - \cos^2\phi_1'\right)}\right)}{\cos^2\phi_1'\left(\tan\beta + \left(\frac{\gamma_t}{\gamma'}\right)k_h - \left(-r_u\right)\tan\phi_{cs}'\right)} \qquad [7]$$

As shown in Eq. (7), in addition to other soil parameters the pore water pressure ratios are required to determine the length l_s. The effects of various parameters in Eq. (7) are discussed in the following sections. A method for estimation of r_u is discussed in Section 7.

6 LENGTH OF WEAK LAYER

Consider a submarine slope having a loose sand layer at a depth of 20 m. The geotechnical parameters for this loose sand are: ϕ_{cs}' = 33º, yield friction angle, ϕ_1' = 28º, γ' = 7 kN/m^3, γ_t = 17 kN/m^3, r_{u1} = 0.5 and β = 5°. The solid lines in Figs. 4 to 6 show the length l_s required for failure of the slope. To explain further consider Fig. 4. If the pore pressure ratio r_u generated from an earthquake near the base of the sliding block is 0.6, the failure is possible if the length of the weak soil layer is at least 165 m. However, if the value of r_u is less than 0.5, failure of the slope is not possible for this geometry and soil conditions, because the frictional resistance along the potential failure plane is sufficient to resist the shear stress. In other words, when r_u is equal to or less than 0.5, a higher value of l_s is strongly required to initiate the slope failure for the above mentioned properties.

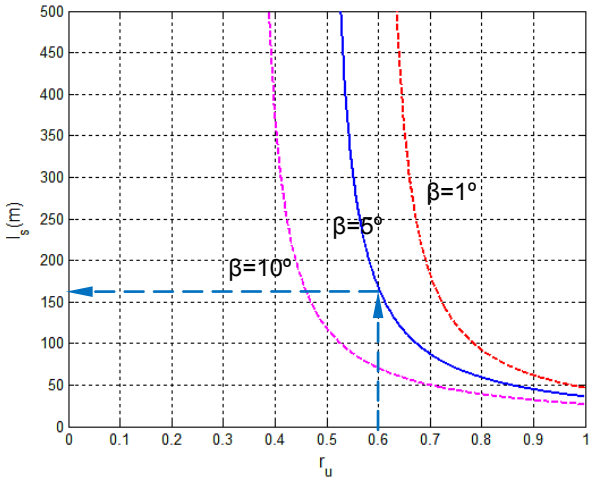

Figure 4: Effects of pore pressure parameter and slope angle, β

In addition to pore pressure ratio, three other parameters are considered to be critical for stability, which are: (i) slope angle, β; (ii) horizontal earthquake coefficient, k_h; and (iii) the depth of the potential sliding surface, d. The effects of these parameters are shown by changing one parameter at a time while keeping the other parameters same as above and shown in Figs. 4 to 6.

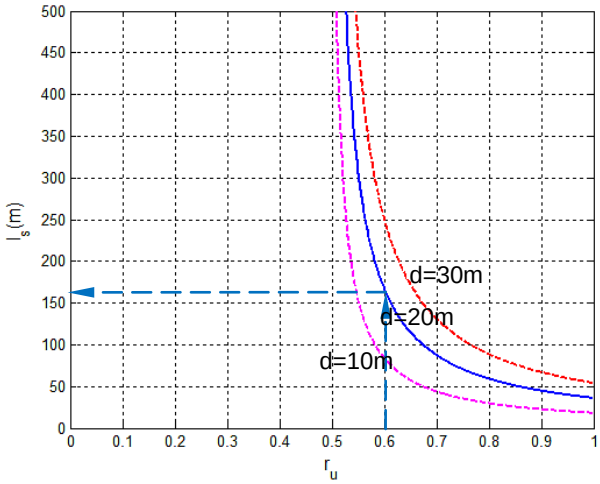

Figure 5: Effect of depth of sand layer, d

The effects of the depth of the sliding surface are shown in Fig. 5. The greater the depth of sliding surface the higher the pore pressure and l_s required to cause the failure of the slope.

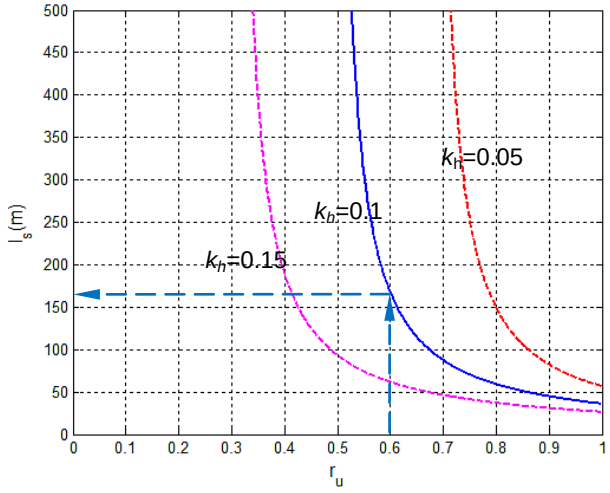

Figure 6: Influence of earthquake coefficient, k_h

Figure 6 shows the effects of k_h, which is related to seismic intensity, on the possibility of failure. As expected, the possibility of failure of a slope is higher for higher values of k_h.

7 ESTIMATION OF EARTHQUAKE INDUCED PORE PRESSURE

As shown above, the earthquake induced pore water pressure has a significant effect on submarine slope failure. Therefore, estimation of r_u is critical in analysis of submarine slope failure.

A number of models have been proposed in the past to estimate the development of excess pore pressure due to earthquake. Zangeneh and Popescu (2003) undertook seismic displacement analyses of submarine slopes using the pore pressure model of Seed and Idriss (1982). In this study, a model based on energy dissipation approach has been chosen for modeling excess pore pressure. The fundamental of the energy-based model is that the increase in pore pressure (Δu) due to an earthquake is a function of dissipated energy (ΔE). The main advantages of this approach are that it is related to both cyclic stress and cyclic strain, and can be related to fundamental earthquake parameters (Kramer 1996). Law et al. (1990) mentioned that the energy dissipation approach is simpler and more reliable. In general, earthquake motions have very different amplitude, frequency content, and duration, and therefore most of the models are empirical and have been developed from statistical analysis of liquefaction case studies. There are similarities and also some differences between the proposed models. However, such comparison is not the aim of this paper and is not presented here; rather the model proposed by Berrill and Davis (1985) has been used.

Davis and Berrill (1982) proposed a model for pore water pressure increase due to earthquake based on 57 case histories. It has been shown that when $r^2\sigma_0'^{3/2}/10^{1.5M}$ is less than $450/N_1^2$ soil liquefaction occurs. Here, N_1 is the corrected SPT-N value, M is the earthquake magnitude, r is the epicentre distance in meter, σ'$_0$ is the initial vertical effective stress in kPa and $r^2\sigma_0'^{3/2}/10^{1.5M}$ is a component related to energy dissipation and pore pressure generation. Further discussion about this component is available in Davis and Berrill (1982). Note that for mild submarine slope (β<10°), σ_0' from Eq. (1) and vertical effective stress are used interchangeably. The variation of $r^2\sigma_0'^{3/2}/10^{1.5M}$ with N_1 is shown by the dashed line in Fig. 7. Based on this Davis and Berrill (1982) proposed a model to calculate the value of r_u as:

$$r_u = \frac{\Delta u}{\sigma_0'} = \frac{450}{r^2 N_1^2 \sigma_0'^{3/2}} 10^{1.5M} \qquad [8]$$

Berrill and Davis (1985) revised and extended their model based on more (90) liquefaction case histories. It has been shown that when $r^2\sigma_0'^{3/2}/\left(A10^{1.5M}\right)$ is less than $\left(20/N_1^{1.5}\right)^2$ soil liquefaction occurs. Here A is the attenuation factor, and other parameters are defined above. The value of A varies between 0.71 and 0.98. Berrill and Davis (1985) also recommended an average value of A equal to 0.9 for this model.

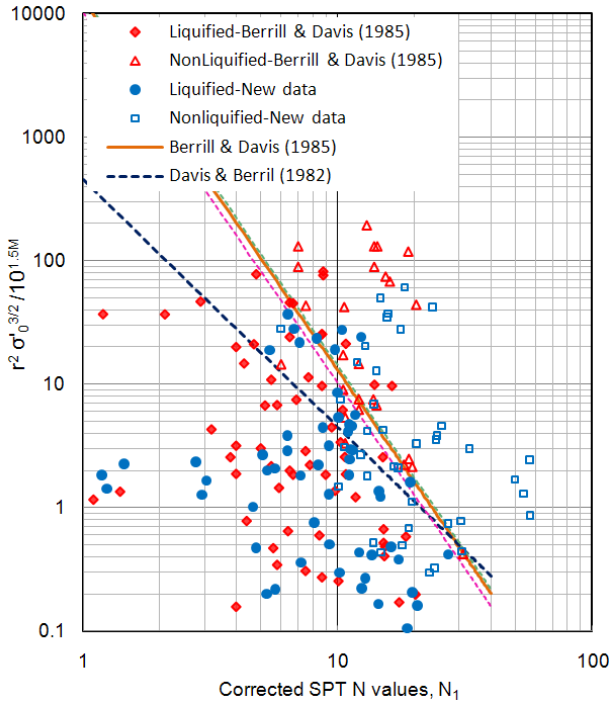

Figure 7: Comparison between liquefaction case history data and energy based models

The solid line in Fig. 7 shows the variation of $r^2\sigma_0'^{3/2}/10^{1.5M}$ with N_1 for A=0.9. The two dashed line near this solid line shows the variation for A=0.71 and 0.98. As shown, the effect of *A* within this range is not significant compared to other parameters.

Berrill and Davis (1985) also revised the pore pressure model as;

$$r_u = \frac{\Delta u}{\sigma_0'} = \frac{120}{N_1^{1.5}} \frac{\sqrt{A}\, 10^{0.75M}}{r\sigma_0'^{0.75}} \qquad [9]$$

In addition to the data used by Berrill and Davis (1985), we have compiled a large number of liquefaction case histories from the literature as plotted in Fig. 7. A total number of 188 case histories obtained from various sources (Berrill and Davis 1985; Law 1990; Seed 1975; and Xie 1984) are plotted in this figure. The additional 98 liquefaction case history data are shown by solid circles for liquefaction and open squares for non-liquefaction. The lines in Fig. 7 show the boundary between liquefied and non-liquefied sites, where the non-liquefied cases are at the right. As shown in Fig.7, the model proposed by Berrill and Davis (1985) better covers liquefaction cases even with additional data. Therefore, Berrill and Davis (1985) model (Eq. 9) has been used in this study to calculate the value of r_u.

8 A WORKED EXAMPLE

Consider a mild submarine slope of β = 5º. Geotechnical parameters are: ϕ'_{cs} = 33º, ϕ'_y = 28º, γ' = 7 kN/m^3, γ_t = 17 kN/m^3, r_{u1} = 0.4 and N_1 = 9. The stability of this slope is required to be analyzed for an earthquake magnitude of 7.5 with an epicentre distance of 75 km. Now using Eq. (9), the pore pressure ratio (r_u) can be calculated with depth. Once the value of r_u is known, the length of the loose sand layer (l_s) can be calculated using Eq. 7. For example, at 20 m depth, r_u = 0.6 and l_s = 200m. That means, if the there is a loose sand layer that extent more than 200m at 20m depth the failure of the slope is possible.

9 CONCLUSIONS

The potential failure of the seabed due to an earthquake is one of the major concerns for the development of offshore facilities. When submarine slope failure involves loose sands, the failure can be governed by both earthquake induced inertia force and excess pore water pressure in the soil.

Both yield and residual shear strength are the critical soil parameters for stability analysis. Once the earthquake induced pore water pressure reduces the effective stress to the yield strength envelope the loose contractive soil is on the verge of collapse and a small trigger may initiate instability of the slope. However, the final failure of the slope is governed by the residual shear strength.

For offshore slope failure the weak sand layers do not have to be continuous. The minimum length required for the failure of a submarine slope can be calculated considering the effects of the forces at the end of the sliding block.

The energy-based model proposed by Berrill and Davis (1985) could be used to estimate earthquake induced pore water pressure. It has been shown that this model performs reasonably well even for additional case histories included in the present study from the literature.

NOTATIONS

The following symbols are used in this paper:

A	: attenuation factor
β	: slope angle
d	: depth of the assumed potential sliding surface
F_s	: factor of safety
k_h	: horizontal earthquake coefficient
l_s	: length required for failure
l_f	: length of the assumed failure plane
M	: earthquake magnitude
N_1	: corrected SPT-N value
ϕ'_{cs}	: friction angle at critical state
ϕ'_y	: friction angle at yield
P_a	: active force
P_p	: passive force
r	: epicentre distance in m
r_u	: excess pore pressure ratio
r_{u1}	: excess pore pressure ratio at yield
τ_g	: gravitational & earthquake induced shear stress
τ_r	: residual shear strength
Δu	: excess pore water pressure at failure
σ'_0	: normal effective stress
γ_t	: total unit weight
γ'	: submerged unit weight

ACKNOWLEDGEMENTS

The writers would like to acknowledge the financial support from Research & Development Corporation of Newfoundland and Labrador and C-CORE.

REFERENCES

Azizian, A. and Popescu, R. 2001. Back analysis of the 1929 Grand Banks submarine slope failure. *Canadian Geotechnical Society Conference*, 808–815.

Berrill, J. B. and Davis, R. O. 1985. Energy dissipation and seismic liquefaction of sands: Revised model. *Soils and Foundations*, 25(2): 106–118.

Biondi, G., Cascone, E., Maugeri, M. and Motta, E. 2000. Seismic response of saturated cohesionless slopes. *Soil dynamics and earthquake engineering*, 20: 209–215.

Brink, U.S.T., Lee, H.J., Geist, E.L. and Twichell D. 2009. Assessment of tsunami hazard to the U.S. East Coast using relationships between submarine landslides and earthquakes. *Marine geology*, 264: 65–73.

Chu, J., Leroueil, S. and Leong, W.K. 2003. Unstable behaviour of sand and its implification for slope instability. *Canadian Geotechnical Journal*, 40: 873–885.

Coulter, S.E. and Phillips, R. 2005. Seismic initiation of submarine slope failures using physical modelling in a geotechnical centrifuge. *Proc. 58th Canadian Geotechnical Conference*, Saskatoon, Paper 588.

Davis, R. O. and Berrill, J. B. 1982. Energy dissipation and seismic liquefaction of sands. *Earthquake engineering and structural dynamics*, 10: 59–68.

Hadj-Hamou, T. and Kavazanjian, E. Jr. 1985. Seismic stability of gentle infinite slopes. *Journal of Geotechnical Engineering*, ASCE, 111(6): 681–697.

Hanzawa, H. 1980. Undrained strength and stability analysis for quick sand. *Soils and Foundation*, 20 (2): 17–29.

Kokusho, T. 2003. Current state of research on flow failure considering void redistribution in liquefied deposits, *Soil Dynamics and Earthquake Engineering*, 23:585–603.

Kramer, S.L.1996. *Geotechnical Earthquake Engineering,* Upper Saddle River, N.J.: Prentice Hall.

Kvalstad, T.J., Andresen, L., Forsberg, C.F., Berg, K., Bryn, P. and Wangen, M. 2005. The Storegga slide: evaluation of triggering sources and slide mechanics. *Marine and petroleum Geology,* 22:245–256.

Law K.T., Cao Y.L. and He, G.N. 1990. An energy approach for assessing seismic liquefaction potential. *Canadian Geotechnical Journal*, 27(3): 320–329.

Lee, H.J., Orzech, K., Locat, J., Boulanger, E., and Konrad, J.M. 2004. Seismic Strengthening, A Conditioning Factor Influencing Submarine Landslide Development. *Proc. 57th Canadian Geotechnical Conference*, 7p.Quebec, Canada.

Locat, J. and Lee, H.J. 2002. Submarine landslides: advances and challenges. *Canadian Geotechnical Journal*, 39: 193–212.

Makdisi, F.I. and Seed, H.B. 1977. A simplified procedure for estimating earthquake-induced deformations in dams and embankments. In: *Rept. UCB/EERC-77/19*, Earthquake Eng. Res. Center.

Masson, D.G., Harbitz, C.B., Wynn, R.B., Pedersen, G. and Løvholt, F. 2006. Submarine landslides: processes, triggers and hazard prediction. *Phil. Trans. R. Soc. A*, 364: 2009–2039.

Mazindrani, Z.H. and Ganjali, M.H. 1997. Lateral earth pressure problem of cohesive backfill with inclined surface. *Journal of Geotechnical and Geoenvironmental Engineering,* ASCE, 123(2): 110–112.

Olson, S.M. and Stark, T.D. 2003. Yield strength ratio and liquefaction analysis of slopes and embankments. *Journal of Geotechnical and Geoenvironmental Engineering,* ASCE, 129(8): 727–737.

Poulos, S.J. 1988. Strength for static and dynamic stability analysis. *Geotechnical Special Publication*, 21: 452–474.

Seed, H.B., Arango, I. and Chan, C.K. 1975. Evaluation of soil liquefaction potential during earthquake. *Earthquake Engineering Research Center*, University of California, Berkley, Report EERC75–28.

Seed, H.B. and Idriss, I.M. 1982. On the importance of dissipation effects in evaluating pore pressure changes due to cyclic loading. *Soil Mechanics – Transient and Cyclic Loads, eds*., Pande, N., Zienkiewics, O.C.: 53–70.

Sladen, J.A., D'Hollanderr, D., and Krai-Inj. 1985. The liquefaction of sands, a collapse surface approach. *Canadian Geotechnical Journal*, 22(4): 564–578.

Terzaghi, K., Peck, R.B. and Mersi, G. 1996. *Soil Mechanics in Engineering Practice,* 3rd edition, John Wiley & Sons, New York.

Vaid, Y.P. and Chern, J.C. 1985. Cyclic and monotonic undrained response of sands. *In Proc. Advances in the Art of Testing Soils under Cyclic Loading*, Detroit, pp. 120–147.

Wright, S.G. and Rathje, E.M. 2003. Triggering mechanisms of slope instability and their relationship to earthquakes and tsunami. *Pure and applied geophysics*, 160: 1865–1877.

Xie, J.F. 1984. Some comments on the formula for estimating the liquefaction of sand in revised a seismic design code. *China Earthquake Engineering and Engineering Vibration,* 2: 95–126.

Yamamuro, J.A. and Lade, P.V. 2011. Evaluation of static liquefaction potential of silty sand slopes. *Canadian Geotechnical Journal*, 48: 247–264.

Yang, J. 2002. Non-uniqueness of flow liquefaction line for loose sand. *Géotechnique,* 52(10): 757–760.

Zangeneh, N. and Popescu, R. 2003. Displacement Analysis of Submarine Slopes using Enhanced Newmark Method. *Proc. 1st Int. Symp. Submarine Mass Movements and their Consequences*, Nice, France, pp.193–204.